Jurnal Teknologi

Full paper

Effect of Surface Texturing Arrangement for Improving Anti-Seizure Property of Lead-Free Copper Alloy

Yuki Kuroiwa[a], Auezhan Amanov[b], Ryo Tsuboi[b], Shinya Sasaki[b*], Shinji Kato[c]

[a]*Graduate School, Tokyo University of Science, 6-3-1 Niijyuku, Katsushika-ku, Tokyo 125-8585, Japan*
[b]*Tokyo University of Science, 6-3-1 Niijyuku, Katsushika-ku, Tokyo 125-8585, Japan*
[c]*KYB Corporation, 1-12-1 Asamizodai, Minami-ku, Kanagawa 252-0328, Japan*

*Corresponding author: s.sasaki@rs.tus.ac.jp

Article history

Received :1 January 2014
Received in revised form :
10 January 2014
Accepted :25 January 2014

Graphical abstract

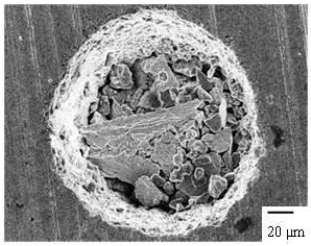

Abstract

Lead-bronze is widely used in the automotive industry owing to its excellent anti-seizure property. However, lead is toxic, and thus, from an environmental viewpoint, there is a demand for a lead-free copper alloy in the automotive industry. Despite the anti-seizure property of lead-free copper alloy being comparable to that of lead-bronze, it has not yet been well exploited. Therefore, the objective of this study was to improve the anti-seizure property of lead-free copper alloy using a laser surface texturing (LST) method. A ring-on-ring sliding friction tester was used to assess the effectiveness of LST and to investigate the effect of surface texturing arrangement on the anti-seizure property of lead-free copper alloy. In the friction tests, upper specimens made of FCD700 and lower specimens made of PBC2 (lead-free copper alloy) were used. Paraffinic oil was used as a lubricant and was circulated using a pump. Results of the friction tests showed that the textured specimens demonstrated superior anti-seizure property to that of the non-textured specimens. Further, on the basis of the obtained experimental results, it was concluded that the arrangement of dimples plays an important role in improving the anti-seizure property of lead-free alloy.

Keywords: Seizure; surface texturing; copper alloy

1.0 INTRODUCTION

Lead-bronze is widely used in the automotive industry because of its excellent anti-seizure property. However, since lead is toxic and can cause severe health problems, there is a demand in this industry for the replacement of lead-bronze with lead-free copper alloy from an environmental viewpoint. However, when lead-free copper alloy is utilized to produce mechanical components, its anti-seizure property is not comparable to that of lead-bronze. When two metal surfaces come into contact in relative motion, seizure occurs once the temperature at their interface reaches a critical temperature [1]. Seizure is accompanied by drastic changes in friction force, wear rate, and surface topography [2]; moreover, it does not occur immediately but develops with increasing sliding time [3].

Surface texturing is a process which allows the fabrication of various precise geometries such as micro-grooves [4], micro-dimples [5], and micro-convexes [6]. Surface texturing can be performed using various methods, such as machining, ion-beam texturing, different types of etching, and laser texturing [7]. Surface texturing has been reported to reduce the friction on account of the textured geometry acting as a reservoir of lubricant and trapping wear debris. In addition, the dimples produced by laser surface texturing (LST) are expected to be beneficial in improving the anti-seizure property of lead-free copper alloy. Therefore, this study was aimed at improving the anti-seizure property of lead-free copper alloy by LST.

The effect of surface texturing on the tribological properties was studied by Koszela *et al.* [8] using a block-on-ring tester, where block specimens were made of bronze (CuSn10P) with a hardness of 138 HB and counter specimens were made of 42CrMo4 steel with a hardness of 40 HRC, and dimples were fabricated on the block surface by a burnishing technique. Results of a seizure resistance test performed in their study at a constant normal load of 2700 N showed that surface texturing was able to increase the lifetime of the analysed assembly by up to five times that of the non-textured surface. Further, Galda *et al.* [9] investigated the effect of surface texturing on the transition of lubrication regimes from mixed to hydrodynamic. In their study, the block specimens were made of EN-GJS 400-15 cast iron of hardness 50 HRC and ring specimens were made of hardened 42CrMo4 steel of hardness 32 HRC; as done in [8], dimples were produced on the block surface by a burnishing technique. Their experimental results revealed that a dimple density smaller than 20% was beneficial for improving the lubrication-regime transitions. Recently, Qiu *et al.* [10] reported the effects of LST on the frictional characteristics of heat-treated 17-4PH stainless steel. In their study, dimples were designed to have different sizes,

densities, and depth-to-diameter ratios. The textured specimens were found to have a lower friction coefficient than the non-textured specimens. However, some of the produced dimples affected the wear resistance. Further, several studies have attempted to investigate the mechanisms and effects of surface texturing on the friction and seizure properties of sliding surfaces [11-13]. However, to the best of our knowledge, no guidelines have been developed for optimizing the design of the geometry and arrangement of dimples that would improve the friction and seizure properties of a sliding surface for a specific application with a replacement of lead-bronze with lead-free copper alloy. Hence, the objective of this study was to confirm the effectiveness of LST in improving the anti-seizure property of lead-free copper alloy and to optimize the geometry and arrangement of dimples for obtaining the lowest friction coefficient and optimum anti-seizure property.

■2.0 EXPERIMENTAL METHODS

A schematic view of the ring-on-ring sliding tester used in this study is shown in Figure 1. The upper rotating specimen was fixed on a motor, whereas the lower stationary specimen was fixed to a cup.

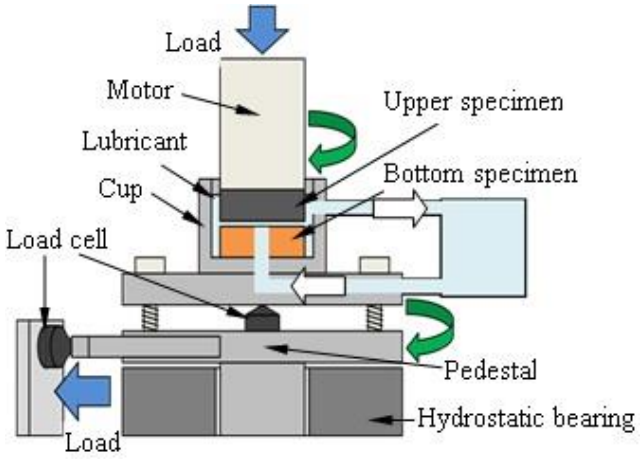

Figure 1 Schematic view of ring-on-ring sliding tester

The upper specimen was pushed towards the lower specimen, and the load and friction torque were measured using a load cell. Daphne Hydraulic Fluid 32 (Idemitsu) paraffinic oil was used as a lubricant (see Table 1 for its physical properties) and was circulated by a pump. The pedestal was supported by a hydrostatic bearing. The upper specimen was made of FCD700, whereas the textured lower specimen was made of PBC2 (lead-free copper alloy) with outer and inner diameters of 44 mm and 27.6 mm, respectively. The average surface roughness (R_a) of both the specimens is about 0.4 µm. It is well known that PBC2 alloy has superior wear resistance and corrosion resistance. It is usually used to manufacture gears, worm gears, bearings, sleeves, impellers, etc. Thus, its anti-seizure property is expected to be improved by LST, after which it can be substituted for lead-bronze. The mechanical properties of FCD700 and PBC2 alloys are listed in Table 2. Two types of tests were conducted in this study: one was aimed at confirming the effectiveness of LST in improving the anti-seizure property of lead-free copper alloy (Test A), and the other was aimed at investigating the effect of surface texturing arrangement on the anti-seizure property (Test B).

Table 1 Physical properties of lubricant

Density	[g/cm³]		0.868
Viscosity	[mm²/s]	@ 20 °C	55.87
		@ 40 °C	31.89
		@ 100 °C	5.456

Table 2 Mechanical properties of FCD700 and PBC2 materials (acquired from JIS G5502 and JIS H5120, respectively)

Material	Tension strength [N/mm²]	Proof strength [N/mm²]	Brinell hardness [HB]
FCD700	≥ 700	≥ 420	180-300HB (10/3000)
PBC2	≥ 195	≥ 120	≥ 60HB (10/1000)

■3.0 EFFECTIVENESS OF LST IN IMPROVING ANTI-SEIZURE PROPERTY OF LEAD-FREE COPPER ALLOY

Table 3 lists the various dimensions, pitches, angles, and area ratios of dimples in Test A; these are also depicted graphically in Figure 2. As seen in this figure, the dimples were arranged radially from the centre of the specimen, on concentric circles. Further, in pattern 1 (Figure 2(a)), the dimples were positioned in a square arrangement relative to each other, whereas in patterns 2 and 3 (Figures 2(b) and (c), respectively), they were positioned in a lattice configuration. Except for the difference in the dimple arrangement, patterns 1 and 2 had the same parameters. Further, patterns 2 and 3 had different area ratios of dimples, as shown in Table 3.

Table 3 Dimple dimensions in Test A

Pattern	Size [µm]	Depth [µm]	Pitch [µm]	Angle [°]	Area ratio [%]
1 Radial (square)	100	100	400	0.36	10.0
2 Radial (lattice)	100	100	160	1.5	9.95
3 Radial (lattice)	100	100	160	3.1	5.0

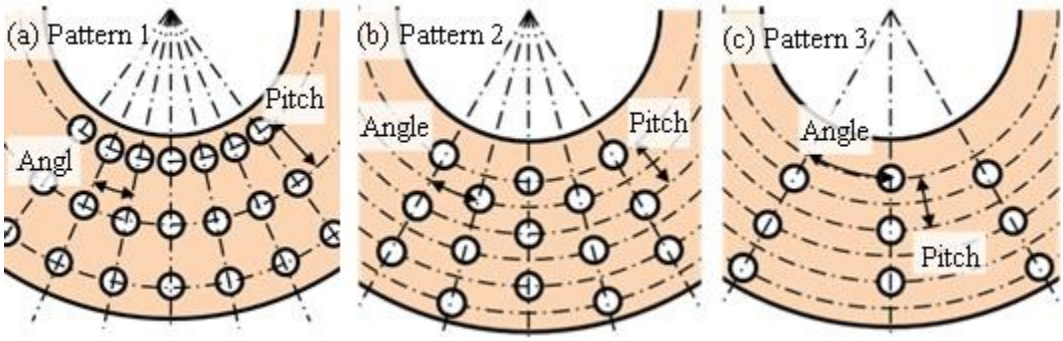

Figure 2 Schematic of dimple arrangement patterns in Test A: (a) pattern 1, (b) pattern 2, and (c) pattern 3

Friction tests were conducted with three different textured specimens (corresponding to patterns 1–3), and their friction and anti-seizure properties were compared to those of the non-textured specimens under an incrementally applied load. The conditions for friction test A are listed in Table 4. The volume of lubricant used in each test was about of 50 ml, which was sufficient to fully immerse the upper specimen in the cup. The sliding friction test was conducted with a running-in period of 10 min at a load of 50 N. Afterwards, the normal load was increased incrementally from 50 N to 1600 N, and the friction coefficient was measured simultaneously.

Table 4 Test A conditions

Rotation speed	[m/s]	0.56
Load	[N]	50 - 1600
Ambient temperature	[°C]	20
Lubricant	[ml]	50

Figure 3 shows the friction coefficients of the non-textured specimen and of specimens with patterns 1, 2, and 3 (hereafter referred to as 'pattern-1 specimen', 'pattern-2 specimen', and 'pattern-3 specimen', respectively) as a function of normal load. In all specimens, the friction coefficient was found to increase at normal loads between 200 N and 400 N. Therefore, another friction test was conducted and halted when the normal load reached 400 N.

Inspection of the surface after the friction test revealed that it did not undergo seizure. Thus, it was concluded that seizure did not occur at a normal load of 400 N. The increase in friction coefficient is considered to be caused by the shift of the lubricated regimes from mixed to boundary. The friction coefficient of all the specimens decreased as the friction test progressed at normal loads higher than 400 N. This decrease in friction coefficient may also be attributed to the surface smoothing.

The average surface roughness (R_a) of all the specimens after the test was about 0.12 µm. Therefore, the surface was considered to have been polished at the boundary lubrication and considerable amount of wear debris was present on the sliding surface. The friction coefficients of the non-textured and pattern-1 specimens increased abruptly at 1200 N and 1100 N, respectively. In the case of the pattern-1 specimen, the friction coefficient attained its maximum value and started decreasing until the friction test ended. In the case of the pattern-2 specimen, the friction coefficient decreased until the friction test ended.

Finally, in the case of the pattern-3 specimen, the friction coefficient increased again at a normal load of 1200 N, but this increase was gradual compared to those of the non-textured and pattern-1 specimens. These results confirmed that the LST improved the friction behaviour of the combination of FCD700 and PCB2 materials.

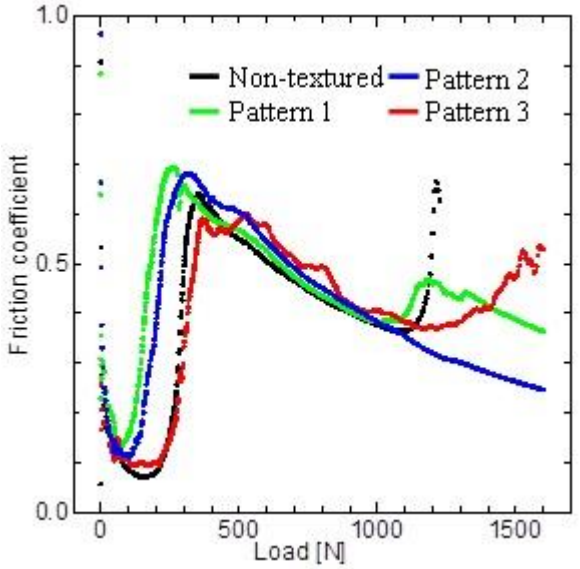

Figure 3 Friction coefficient of non-textured, pattern-1, pattern-2, and pattern-3 specimens as a function of load

Figure 4 shows the optical microscopy (OM) images of the non-textured and textured lower specimens after the friction test. As shown in Figure 4(a), the wear observed in the non-textured specimen was not as severe as that in the textured specimens, since the friction test was halted at a normal load of about 1200 N because of the high friction at this load. From Figures 4(b) and (d), it is evident that the dimples had disappeared in pattern-1 and pattern-3 specimens, which may be attributed to the severe wear in these specimens. These results demonstrate that seizure and severe wear occurred in specimens with patterns 1 and 3. However, in the pattern-2 specimen (Figure 4(c)), seizure did not occur, since the wear on the surface was not severe. The

observed superior anti-seizure property of the pattern-2 specimen to that of the pattern-1 specimen may be attributed to the large number of dimples at the contact interface in the former; further, the observed superior anti-seizure property of the pattern-2 specimen to that of the pattern-3 specimen may be attributed to the difference in angles and area ratios of these two specimens.

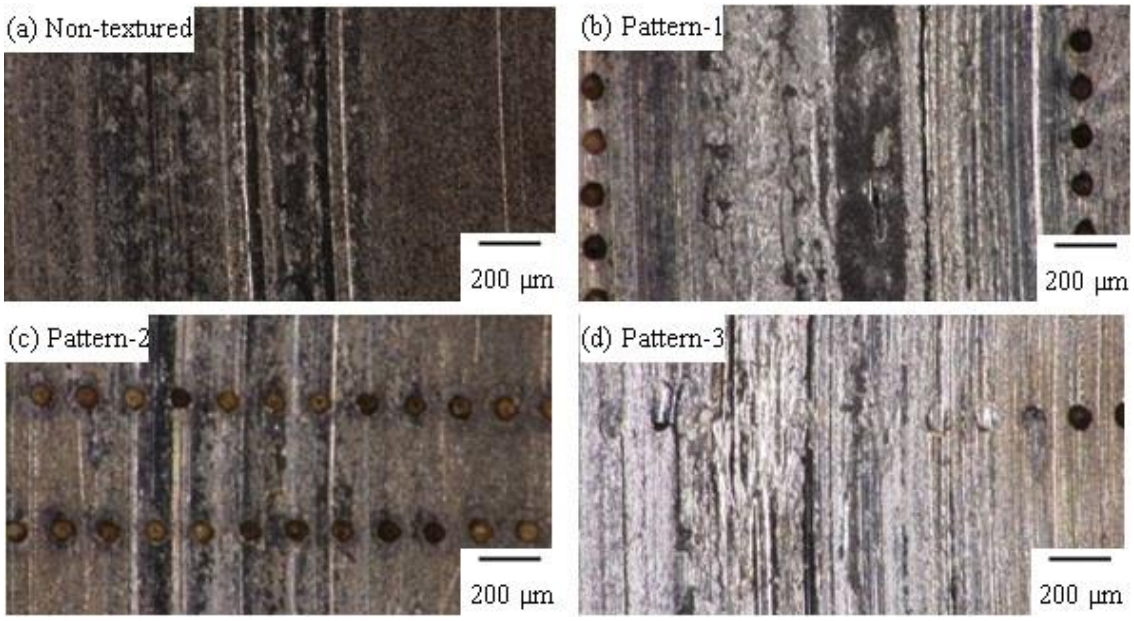

Figure 4 OM images of non-textured (a), pattern-1 (b), pattern-2 (c), and pattern-3 (d) PBC2 specimens after friction test for about 4 min (1200 N) and 5 min (1600 N)

Figure 5 shows cross-sectional profiles of the wear track measured using a laser microscope. The non-textured specimen showed scratch traces at a depth of 5 μm. Further, the pattern-2 specimen showed shallow dimples. The maximum depth of the wear trace was 25 μm, which was shallower than the initial depth of the dimple (100 μm). Finally, the pattern-1 and pattern-3 specimens showed wear traces that were much larger than the initial diameter of the dimple (100 μm). Outside of the wear track in the pattern-1 specimen, the dimple depth remained the same as that before the test. Therefore, it is considered that dimples did not disappear by wear, but rather by trapping of the wear debris. Following the friction tests, no effect of LST was observed in the pattern-1 and pattern-3 specimens, since the dimples were filled with wear debris and particles. Figure 6 shows the scanning electron microscopy (SEM) image of a single dimple of the pattern-2 specimen after the friction test. It can be clearly seen that wear debris was trapped in the dimple.

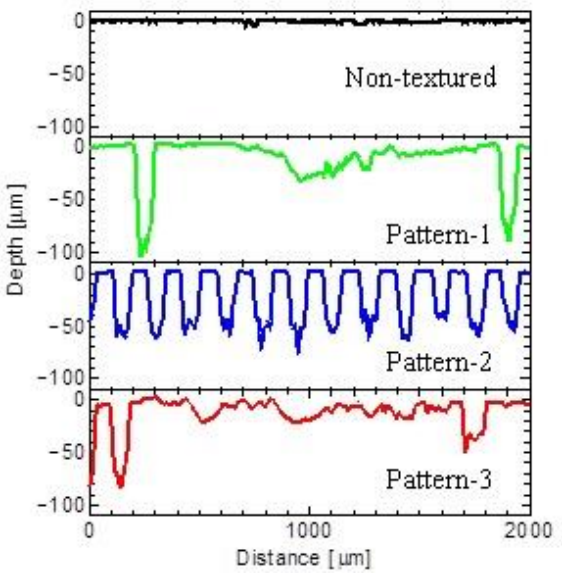

Figure 5 Cross-sectional profiles of non-textured, pattern-1, pattern-2, and pattern-3 PBC2 specimens after friction tests for 4 and 5 minutes

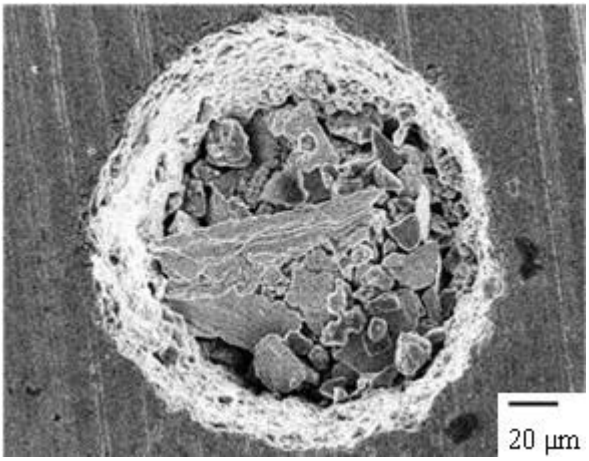

Figure 6 SEM image of pattern-2 specimen

Figure 7 shows the energy-dispersive X-ray spectroscopy (EDS) images of the FCD700 upper specimens that slid against the lower non-textured, pattern-1, pattern-2, and pattern-3 PBC2 specimens. Adhesive wear was observed to occur on the specimen surfaces that slid against the pattern-1 and pattern-3 specimens. Some adhesive wear was also observed on the specimen surfaces that slid against the non-textured and the pattern-2 specimens. In the specimen surfaces that slid against the pattern-1 and pattern-3 specimens, strong adhesion was observed on the wear track, but the adhesion was not so strong on the specimen surfaces that slid against the pattern-2 specimen. This difference in adhesive wear is considered to be caused by the occurrence of seizure in the pattern-1 and pattern-3 specimens.

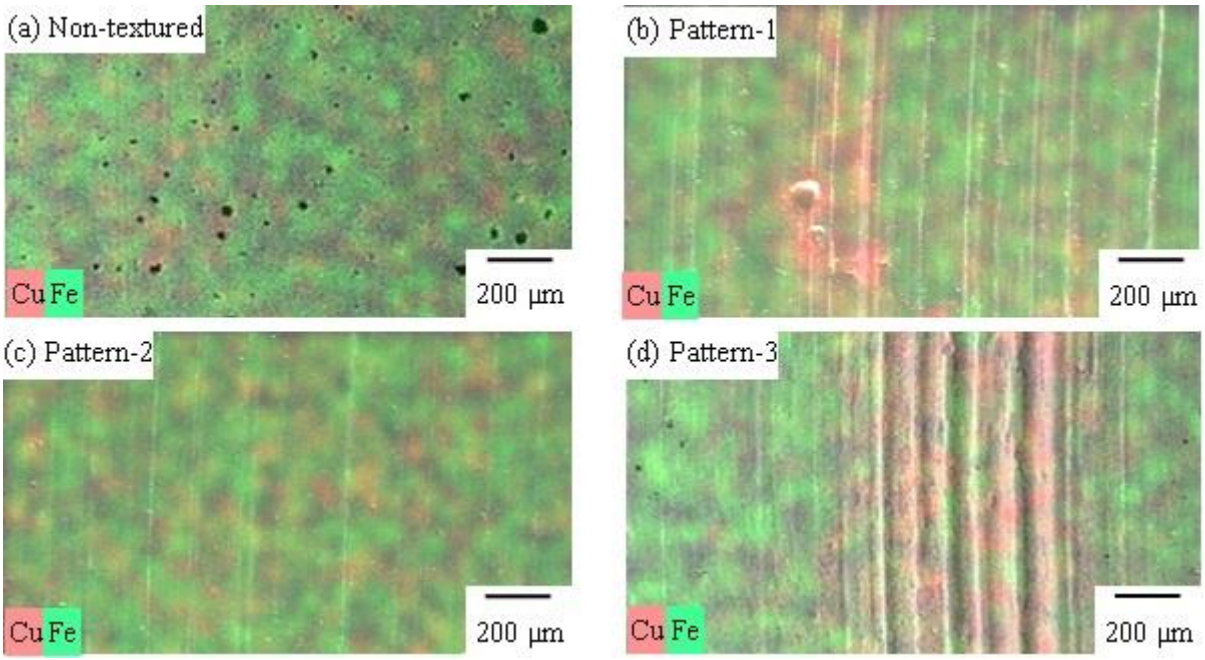

Figure 7 EDS images of FCD specimens that slid against non-textured (a), pattern-1 (b), pattern-2 (c), and pattern-3 (d) PBC2 specimens after friction test

After the friction test, the FCD700 specimens were analysed using an EDS system, with the results as shown in Figure 8. A small amount of Cu was detected in all the FCD700 specimens, which was transferred from the lower specimen of PBC2. The smallest amount of Cu was present in the FCD700 specimen that slid against the pattern-2 specimen. Therefore, the adhesive wear was considered to be controlled by the design of the dimple geometry and arrangement. These results demonstrate the effectiveness of LST in the improvement of the anti-seizure property of the pattern-2 specimen. The experimental results also demonstrate that the arrangement and area ratio of the dimples play an important role in improving the anti-seizure property.

Cross-sectional profiles of the wear tracks generated on the FCD700 specimens are shown in Figure 9. Shallow scratch traces were observed on specimens that slid against the non-textured and pattern-2 specimens. In contrast, 10-μm-deep wear traces were observed on the sliding surfaces of specimens that slid against the pattern-1 and pattern-3 specimens. Comparison of the specimens that slid against the pattern-1 and pattern-3 specimens revealed that the wear traces on the specimen that slid against the pattern-3 specimen are wider than those against the pattern-1 specimen. However, the depth of the wear traces on the specimen that slid against the pattern-3 specimen is shallower than that on the specimen that slid against the pattern-1 specimen. For this reason, it is difficult to estimate which parameter is more effective in improving the anti-seizure property.

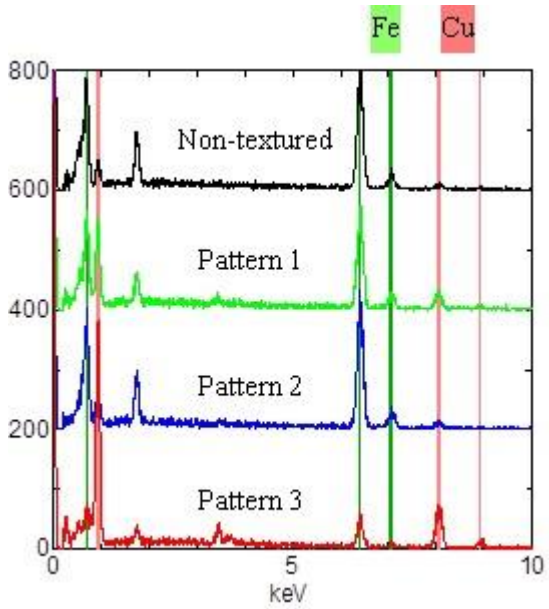

Figure 8 EDS analysis of FCD700 specimens after friction test

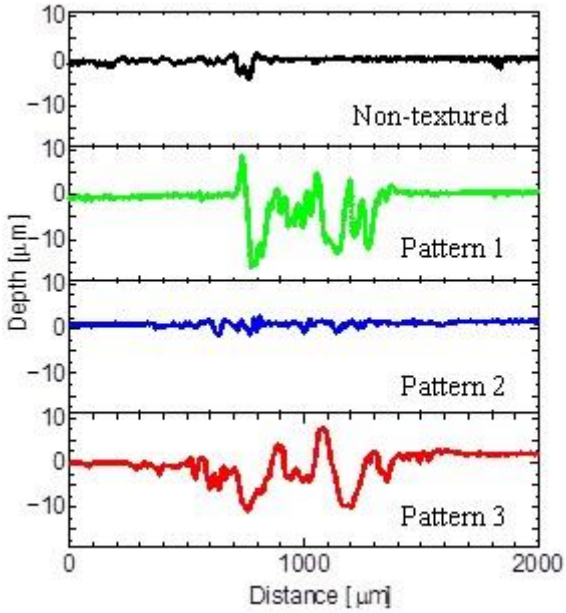

Figure 9 Cross-sectional profiles of wear tracks on FCD700 specimens that slid against non-textured, pattern-1, pattern-2, and pattern-3 PBC2 specimens after friction test

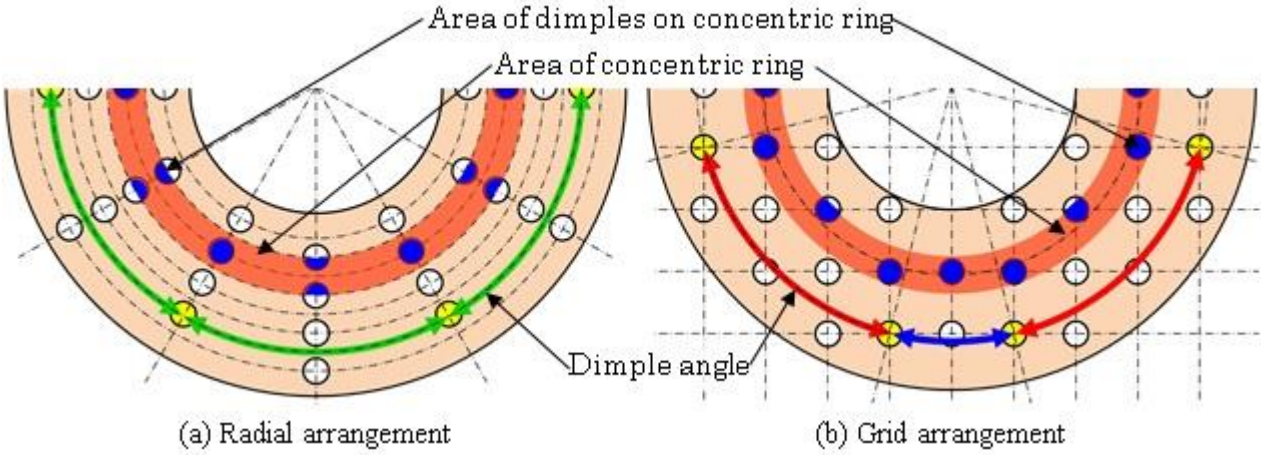

Figure 10 Schematic view of dimple ratio and dimple angle in radial and grid arrangements

■4.0 EFFECT OF DIMPLE (SURFACE TEXTURING) ARRANGEMENT ON ANTI-SEIZURE PROPERTY

In many previous studies, dimples were arranged in a radial or grid layout. However, these arrangements are considered to have different geometrical characteristics. To validate the argument on the difference between these dimple arrangements, two parameters related to dimple arrangement are defined in this study. One is ‘dimple ratio’, which is defined as ‘the area of dimples on the concentric ring divided by the area of the concentric ring’. The other is ‘dimple angle’, which is defined as ‘the angle between two adjacent dimples on the same concentric circle’. Figure 10 shows a schematic view of the dimple ratio and dimple angle in the radial and grid arrangements. This figure shows that the dimple angle is constant in the radial arrangement and that the dimple angle is not constant in the grid arrangement.

Figure 11 shows the distribution of the dimple ratio in the radial and the grid arrangements. It is seen that the dimple ratio in the radial arrangement decreases with increasing radius of the concentric ring. In contrast, the dimple ratio in the grid arrangement is independent of the radius amplitude. Since these arrangements have different characteristics as described above, a new arrangement is considered next: a spiral arrangement, wherein the dimple angle is constant and the dimple ratio is independent of the radius amplitude.

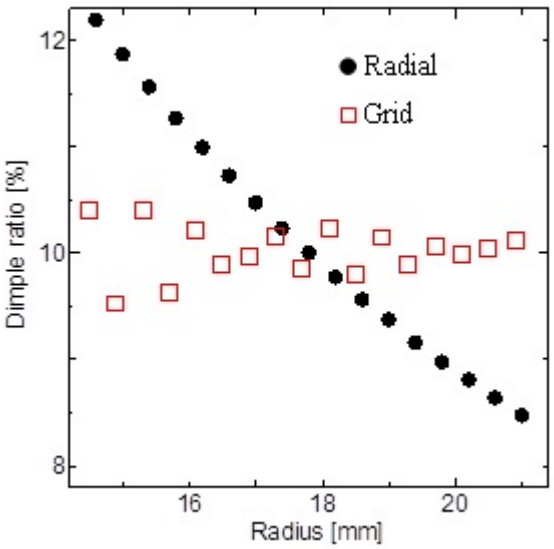

Figure 11 Distribution of dimple ratio in radial and grid arrangements

Figure 12 shows the schematic of the spiral arrangement. A single spiral line is defined as follows:

$R = \alpha\theta$,
$Pitch = \int\alpha(1+\theta^2)^{1/2}d\theta$ (α: arbitrary constant)

Here, R is the distance from the centre of the specimen, α is the distance between the orbits of spirals (arbitrary constant), θ is the angle from a reference point (at an inner dimple) on a single spiral line, and *pitch* is the distance between adjacent dimples on the same spiral line.

First, the value of α was defined to decide the form of the single spiral line. Next, the *pitch* value between the dimples was defined to set the number of dimples on the single spiral line. Subsequently, the area ratio was defined as being 10% in this case. From α, *pitch*, and the area ratio, the number of spiral lines was obtained. Then, the calculated spiral lines were placed at equal angles. This process gave a constant dimple angle.

Table 5 lists the dimple dimensions, *pitch*, dimple angles, α, and area ratios in Test B, which investigated the effect of surface texturing arrangement on the anti-seizure property. In all cases, the area ratio was about 10%. In the radial arrangement, the parameters were the same as those of the pattern-2 specimen in Test A. In the grid arrangement, *pitch* was defined by the area ratio because the dimples were arranged in squares.

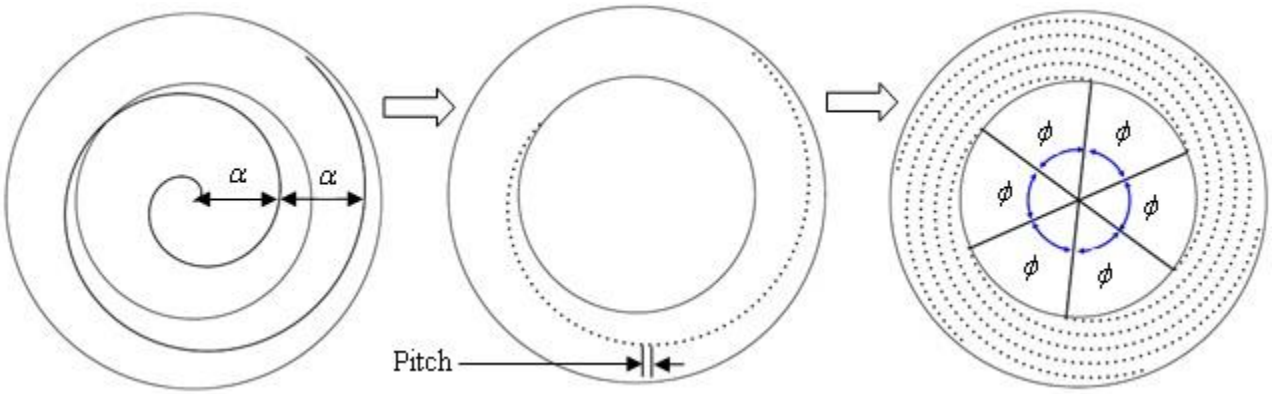

Figure 12 Schematic and process of forming spiral arrangement

Table 5 Dimple dimensions in Test B

Pattern	Size [μm]	Depth [μm]	Pitch [μm]	Angle [°]	α	Area ratio [%]
Radial	100	100	160	1.5	-	9.95
Grid	100	100	282	-	-	10.0
Spiral	100	100	282	-	2.8	9.88

Figure 13 shows the distribution of the dimple ratio in the spiral arrangement. This figure confirms that in the spiral arrangement, the dimple ratio is independent of the radius amplitude.

Friction tests were conducted with three different textured specimens—grid, radial, and spiral—and their friction and anti-seizure properties were compared (Test B). The friction test conditions are listed in Table 6. The sliding friction test was conducted with a running-in period of 10 min at a load of 50 N. Afterwards, the normal load was increased incrementally from 50 N to 1800 N; it was then maintained at 1800 N for 30 min and the friction coefficient was measured simultaneously.

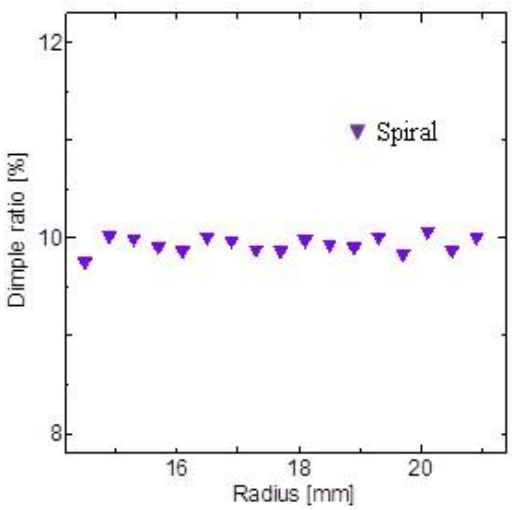

Figure 13 Distribution of dimple ratio in spiral arrangement

Table 6 Test B conditions

Rotating speed	**[m/s]**	**0.37**
Load	[N]	1800
Ambient temperature	[°C]	20
Lubricant	[ml]	Circulating

Figure 14 shows the time histories of the friction coefficients in the radial, grid, and spiral specimens with a normal load of 1800 N. This figure reveals that the friction coefficient of the radial specimens increased abruptly and that the friction coefficient of the grid and spiral specimens was about 0.12 and it did not increase.

Figure 15 shows the SEM images of the textured specimens after the friction test. From this figure and the rapid increase in the friction coefficient in Fig. 14, it is confirmed that seizure occurred in the specimen with the radial arrangement, and this seizure was located in the outer region of the ring.

Table 7 presents a summary of the characteristics and corresponding results for each arrangement. This table reveals that the friction coefficient is almost the same in the grid and spiral arrangements. However, the dimple angles are different in these arrangements. This result suggests that the dimple angle does not affect the anti-seizure property. The three arrangements differ in terms of the distribution pattern of the dimple ratio. Therefore, it is suggested that the distribution of the dimple ratio affects the anti-seizure property.

Table 7 Summary of characteristics and corresponding results for the three surface texturing arrangements

Pattern	**Dimple ratio distribution**	**Dimple angle**	**Friction coefficient (Ave.)**	**Time of seizure (Ave.)**
Radial	Depends on radius	Constant	-	385
Grid	Independent of radius	Inconsistent	0.125	-
Spiral	Independent of radius	Constant	0.120	-

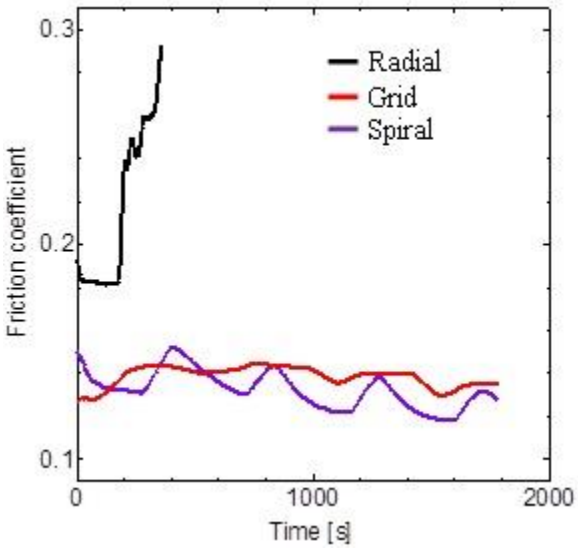

Figure 14 Variation in friction coefficient of radial, grid, and spiral specimens under 1800 N load

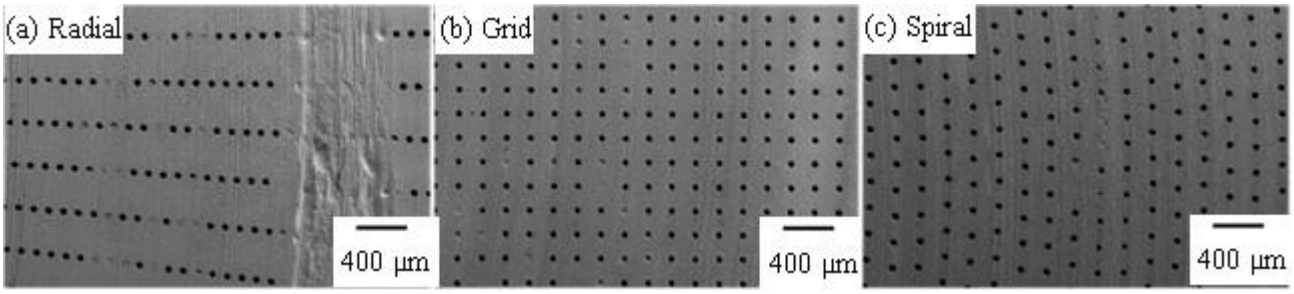

Figure 15 SEM images of textured lower specimens after friction test

5.0 CONCLUSION

In this study, the effectiveness of laser surface texturing (LST) in improving the anti-seizure property of lead-free copper alloy was investigated; additionally, the effect of surface texturing arrangement on the anti-seizure property was also evaluated experimentally through friction tests. The experimental results confirmed that LST successfully improved the friction and anti-seizure properties of lead-free copper alloy. Further, the arrangement and area ratio of the dimples fabricated on the sliding surface were found to play an important role in improving the anti-seizure property of the alloy. Wear debris was seen to be trapped in the dimples after the friction test. Further, adhesive wear was observed on the surfaces of all the FCD700 specimens that slid against the non-textured specimen as well as the three different textured specimens. However, this wear was small on the FCD700 specimen surface that slid against a specimen in which dimples were arranged in a lattice configuration with an area ratio of 10%. Further, the distribution of the dimple ratio in the direction of the radius of the concentric ring on which the dimples are arranged in the radial arrangement was shown to affect the anti-seizure property of the alloy. Further, the anti-seizure property was found to be independent of the stability of the dimple angle. Finally, spiral arrangement was showed the lowest friction coefficient of three arrangements.

Acknowledgement

This work was supported by a grant from JSPS KAKENHI (No. 23360077).

References

[1] Stachowiak, G., Batchelor, A. W. 2005. *Engineering Tribology*. Third Edition. Butterworth-Heinemann, Oxford, U.K.
[2] Ruff, A. W., Bayer, R. G. 1993. Tribology: Wear Test Selection for Design and Application, ASTM International, West Conshohocken, U.S.A.
[3] Markov, D., Kelly, D. 2000. Mechanisms of Adhesion-initiated Catastrophic Wear: Pure Sliding. *Wear*. 239: 189.
[4] Yuan, S., Huang, W., Wang, X. 2011. Orientation Effects of Micro-Grooves on Sliding Surfaces. *Tribology International*. 44: 1047.
[5] Li, J., Xiong, D., Dai, J., Huang, Z., Tyagi, R. 2010. Effect of Surface Laser Texture on Friction Properties of Nickel-Based Composite. *Tribology International*. 43: 1193.
[6] Nakano, M., Miyake, K., Korenaga, A., Sasaki, S., Ando, Y. 2009. Tribological Properties of Patterned NiFe-covered Si Surfaces. *Tribology Letters*. 35: 133.
[7] Etsion, I. 2004. Improving Tribological Performance of Mechanical Components by Laser Surface Texturing. *Tribology Letters*. 17: 733.
[8] Koszela, W., Galda, L., Dzierwa, A., Pawlus, P. 2010. The Effect of Surface Texturing on Seizure Resistance of a Steel–Bronze Assembly. *Tribology International*. 43: 1933.
[9] Galda, L., Pawlus, P., Sep, J. 2009. Dimples Shape and Distribution Effect on Characteristics of Stribeck Curve. *Tribology International*. 42: 1505.
[10] Qiu, Y., Khonsari, M. M. 2011. Experimental Investigation of Tribological Performance of Laser Textured Stainless Steel Rings. *Tribology International*. 44: 635.
[11] Wang, X., Kato, K. 2002. Improving the Anti-seizure Ability of SiC Seal in Water with RIE Texturing. *Tribology Letters*. 14: 275.
[12] Yan, D., Qu, N., Li, H., Wang, X. 2010. Significance of Dimple Parameters on the Friction of Sliding Surfaces Investigated by Orthogonal Experiments. *Tribology Transactions*. 53: 703.
[13] Grabon, W., Koszela, W., Pawlus, P., Ochwat, S. 2013. Improving Tribological Behavior of Piston Ring-cylinder Liner Frictional Pair by Liner Surface Texturing. *Tribology International*. 61: 102.